

Intrinsic dynamic shapes responses to external stimulation in the human brain

Reviewed Preprint

v1 • February 27, 2025

Not revised

Maximilian Nentwich , Marcin Leszczynski, Charles E Schroeder, Stephan Bickel, Lucas C Parra

The Feinstein Institutes for Medical Research, Northwell Health, Manhasset, United States • Departments of Psychiatry and Neurology, Columbia University College of Physicians and Surgeons, New York, United States • Translational Neuroscience Lab Division, Center for Biomedical Imaging and Neuromodulation, Nathan Kline Institute, Orangeburg, United States • Cognitive Science Department, Institute of Philosophy, Jagiellonian University, Kraków, Poland • Departments of Neurology and Neurosurgery, Zucker School of Medicine at Hofstra/Northwell, Hempstead, United States • Center for Biomedical Imaging and Neuromodulation, Nathan Kline Institute, Orangeburg, United States • Department of Biomedical Engineering, The City College of New York, New York, United States

 https://en.wikipedia.org/wiki/Open_access Copyright information

eLife Assessment

This manuscript presents an interesting new framework (VARX) for simultaneously quantifying effective connectivity in brain activity during sensory stimulation and how that brain activity is being driven by that sensory stimulation. The reviewers thought the model was original and its conclusion that intrinsic connectivity is largely unaltered during sensory stimulation is very interesting, but that future use of the model could potentially be affected by false positive conclusions. Overall, this work is **important** with **solid** evidence for its conclusions - it will be of interest to neuroscientists working on brain connectivity and dynamics.

<https://doi.org/10.7554/eLife.104996.1.sa2>

Abstract

Summary

Sensory stimulation of the brain reverberates in its recurrent neuronal networks. However, current computational models of brain activity do not separate immediate sensory responses from intrinsic recurrent dynamics. We apply a vector-autoregressive model with external input (VARX), combining the concepts of “functional connectivity” and “encoding models”, to intracranial recordings in humans. We find that the recurrent connectivity during rest is largely unaltered during movie watching. The intrinsic recurrent dynamic enhances and prolongs the neural responses to scene cuts, eye movements, and sounds. Failing to account for these exogenous inputs, leads to spurious connections in the intrinsic “connectivity”. The model shows that an external stimulus can reduce intrinsic noise. It also shows that sensory areas have mostly outward, whereas higher-order brain areas mostly incoming connections.

We conclude that the response to an external audiovisual stimulus can largely be attributed to the intrinsic dynamic of the brain, already observed during rest.

Introduction

The primate brain is highly interconnected between and within brain areas. This includes areas involved in sensory processing ¹. Strikingly, most computational models of brain activity in response to external natural stimuli do not take the recurrent architecture of brain networks into account. “Encoding” models often rely on simple input/output relationships such as general linear models in fMRI ², or temporal response functions in EEG/MEG ³. Interactions between brain areas are captured often just as instantaneous linear correlations that are referred to as “functional connectivity” when analyzing fMRI activity ⁴. Others capture synchronous activity in different brain areas by measuring phase locking of electrical neural signals ⁵. However, these measures of instantaneous correlation do not capture time delays inherent in recurrent dynamics. By taking temporal precedence into account with recurrent models the “Granger-causality” formalism can establish directed “connectivity”. This has been used to analyze both fMRI and electrical activity ^{6–11}.

The concept of functional connectivity was first developed to analyze neural activity during rest, where there are no obvious external signals to stimulate brain activity. But it is now also often used during passive exposure to a stimulus, such as watching movies ^{12–15}. A general observation of these studies is that a portion of the functional connectivity is preserved between rest and stimulus conditions, while some aspects are altered by the perceptual task, e.g. ^{12,16}. This should be no surprise, given that an external stimulus can drive multiple brain areas and thus induce correlations between these areas ¹⁷. Removing such stimulus-induced correlations by controlling for a common cause is standard practice in statistical modeling and causal inference ¹⁸. However, in studies that focus on functional connectivity in neuroscience, stimulus-induced correlations are often ignored when analyzing the correlation structure of neural signals. A notable exception is “dynamic causal modeling” ¹⁹. In this modeling approach the “input” can modulate functional connectivity. This is particularly important in the context of active behavioral tasks, where the common finding is that correlation structure changes with task states ²⁰.

In this study we are interested in “passive” tasks such as rest and movie watching. We will ask here whether, after removing stimulus-induced correlations, the intrinsic dynamic itself is preserved. Attempts to factor out the effects of the stimulus come from work on response variability. For instance, fMRI shows that variability across trials in motor cortex is due to an intrinsic “noise” which is linearly superimposed on a more reliable response to a simple motor action ²¹. Stimulus-response variability in the visual cortex has been attributed to variability of ongoing dynamic ^{22,23}. Some studies of electrical recordings from the visual cortex show that correlations of spiking activity between different recording locations are largely unaffected by visual stimulation ²⁴. Yet, other studies show that visual input affects local correlation in the visual cortex ^{25–27} and across the brain ²⁸.

The technical challenge when addressing these questions is to separate the direct effect of the stimulus from the intrinsic recurrent dynamic. Here we propose to separate these effects by modeling them simultaneously with the simplest possible model, namely, linear intrinsic effects between brain areas and linear responses to extrinsic input. A mathematical model that implements this is the vector-autoregressive model with external input (VARX). This model is well established in the field of linear systems ²⁹ and econometrics ³⁰, where it is used to capture intrinsic dynamics in the presence of an external input. The VARX model is an extension of the VAR model that is routinely used to establish “Granger-causality” in neuroscience (cited above). In

the VARX model, Granger analysis provides a measure of statistical significance for the intrinsic dynamic as well as the external input, in addition to directionality for the intrinsic effects, all as part of a single model [31](#).

While linear systems are an inadequate model of neuronal dynamics, they remain an important tool to understand neural representations because of their conceptual simplicity. They are routinely used for event-related fMRI analysis but also for “encoding models” to link non-linear features of continuous stimuli to neural responses. They have been used to analyze responses to video in fMRI [32](#), to speech in EEG [33](#) or to audio in intracranial EEG [34](#). They are even used to analyze the encoding in deep-neural network models [35](#). Here we use a classic linear model to combine two canonical concepts in neuroscience, which have thus far remained separated, namely, that of “encoding models” [32](#) and “functional connectivity” models [6](#). We will use this to analyze whole-brain, intracranial EEG in human subjects at rest, and while they watch videos. Our main finding is that the recurrent dynamic observed during rest is only minimally altered by watching videos. Instead, the brain’s response to naturalistic stimulus appears to be substantially shaped by the same endogenous dynamic of the brain observed during rest.

Methods

The vector-autoregressive model with external input (VARX) falls within a group of well-established linear models used in neuroscience (see **Table 1** [31](#)). Prominent examples in this group are the generalized linear model (GLM), dynamic causal model (DCM) and temporal response functions (TRF). While these models have been extensively used for neural signal analysis, the VARX model has not. We start therefore with a brief introduction. For more details please refer to [31](#).

VARX model

The VARX model explains a time-varying vectorial signal $y(t)$ as the result of an intrinsic autoregressive feedback driven by an innovation process $e(t)$ and an extrinsic (We adopt here the terminology of “Intrinsic” and “extrinsic” as it is commonly used in neuroscience and psychology. In system modeling and econometrics, where the VARX model is prevalent, the more common terminology is “endogenous” and “exogenous”, meaning effectively the same thing) input $x(t)$:

$$y(t) = \mathbf{A} * y(t - 1) + \mathbf{B} * x(t) + e(t)$$

\mathbf{A}^* and \mathbf{B}^* represent convolutions with appropriately sized matrices of causal filters with lengths n_a and n_b respectively. The innovation is assumed to be uncorrelated in time and has therefore a uniform spectrum. The recurrence in \mathbf{A} modifies this spectrum to match the spectrum of $y(t)$, thereby capturing the intrinsic recurrent dynamic. The filter \mathbf{B} injects a filtered version of the extrinsic input $x(t)$ into this recurrent dynamic. The role of each of these terms for brain activity is explained in **Fig. 1** [31](#).

Filter matrices \mathbf{A} and \mathbf{B} are unknown and can be estimated from the observed history of $x(t)$ and $y(t)$ using ordinary least squares (OLS). The objective for the optimal model is to minimize the power of the unobserved innovation process $e(t)$:

$$\sigma^2 = 1/T \sum_{t=1}^T e(t)^2$$

Model	Intrinsic effect A	Extrinsic effect B	Interact	Delay n_a, n_b	Estimation speed	Reference, with code where available
GLM	no	yes	no	=1	medium	⁴⁰ , SPM, FSL
DCM	yes	yes	yes ²	=1 ³	slow	¹⁹ , no code
VAR	yes	no	no	>1	fast/slow	⁴¹
mTRF	no	yes	no	>1	fast	³⁹
VARX	yes	yes	no ⁴	>1	fast	³¹

Table 1

Models commonly used in neural signal analysis

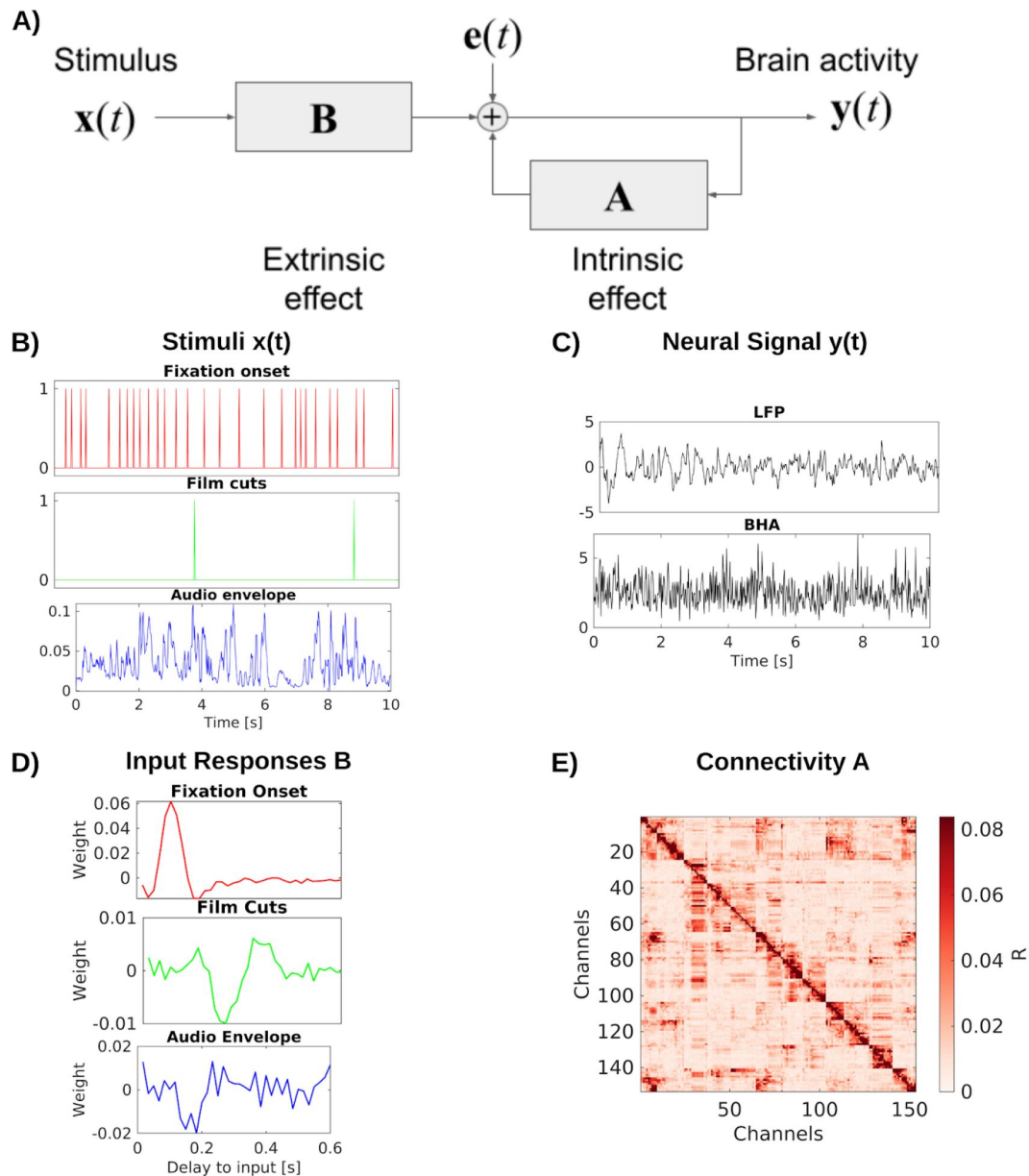


Figure 1

VARX model of the brain:

A) Block diagram of VARX model. $y(t)$ represents observable neural activity in different brain areas, $x(t)$ are observable features of a continuous sensory stimulus, A represent the recurrent connections within and between brain areas (intrinsic effect), and B captures the transduction of the sensory stimuli into neural activity and transmission to different brain areas (extrinsic effect). The diagonal term in A captures recurrent feedback within a brain area. Finally, $e(t)$ is unobserved intrinsic “random” brain activity. B) Example of input stimulus features $x(t)$. C) Single channel examples of neural signal $y(t)$. D) Examples of moving-average response filters B . E) Effect size R for the “connections” captured by auto-regressive filters A .

Granger analysis

The innovation is also the prediction error, for predicting $y(t)$ from the past $y(t-1)$ and input $x(t)$. In the Granger formalism the prediction error is calculated with all predictors included (error of the full model, σ_f) or with individual dimension in $y(t-1)$ or $x(t)$ omitted (error of the reduced models, σ_r)³⁶. To quantify the “effect” of the specific dimension one can take the ratio of these errors³⁷ leading to the test statistic D known as the “deviance”. When the number of samples is T large, the deviance follows the Chi-square distribution with cumulative density F , from which one can compute a p-value:

$$\begin{aligned} D &= T \log(\sigma_r^2 / \sigma_f^2) \\ p &= 1 - F(D, T) \\ R^2 &= 1 - \exp(-D/T) \end{aligned}$$

The p-value quantifies the probability that a specific connection in A or B is zero. The “generalized” R^2 ³⁸ serves as a measure of effect size, capturing the strength of each connection (D , p and R can be computed for each connection in matrix A or B). While this Granger formalism is well established in the context of estimating, A i.e. VAR models, to our knowledge, it has not been used in the context of estimating B, i.e. VARX or TRF models.

Overall system response

The overall brain response to the stimulus for the VARX model is given by the system impulse response (written here in the z-domain, or Fourier domain):

$$\mathbf{H} = (\mathbf{I} - \mathbf{A})^{-1}\mathbf{B}$$

What we see here is that the system response \mathbf{H} is factorized into an autoregressive (AR) filter and \mathbf{A} a moving average (MA) filter \mathbf{B} . When modeled as a single MA filter, the total system response has been called the “multivariate Temporal Response Function” (mTRF) in the neuroscience community³⁹. We found that the VARX estimate of \mathbf{H} is nearly identical to the estimated mTRF³¹. In other words, \mathbf{B} and \mathbf{A} are a valid factorization of the mTRF into immediate extrinsic versus recurrent intrinsic effects.

Note that the extrinsic effects captured with filters \mathbf{B} are specific (every stimulus dimension has a specific effect on each brain area), whereas the endogenous dynamic propagates this initial effect to all connected brain areas via matrix, \mathbf{A} effectively mixing and adding the responses of all stimulus dimensions. Therefore, this factorization separates stimulus-specific effects from the shared endogenous dynamic.

Relation to common neural signal models

The VARX model fits naturally into the existing family of models used for neural signals analysis (Table 1). While they differ in the formulation and statistical assumptions, their defining equations have a similar general form with the following attributes:

An important simplifying assumption for the mTRF, VAR, and VARX models is that $\mathbf{y}(t)$ is observable with additive normal distributed innovation. As a result, parameter estimation can use ordinary least squares, which is fast to compute. In contrast, GLM, DCM, and some variants of VAR models assume that $\mathbf{y}(t)$ is not directly observable, and needs to be estimated in addition to the unknown parameters \mathbf{A} or \mathbf{B} . The same is true for the basic “output error” model in linear systems theory²⁹. This requires slower iterative algorithms, such as expectation maximization. As a result, these models are often limited to small networks (The original DCM proposed for fMRI included an added complication of modeling the hemodynamic response, which amounts to

adding a temporal filter to each output node and prior to adding observation noise.) of a few nodes to test specific alternative hypotheses [42](#). In contrast, here we will analyze 100-200 channels per subject to draw general conclusions about overall brain organization.

Validation of connectivity estimate on whole-brain neural mass model

To validate the interpretation that A is a model of “connectivity”, we simulated neural activity for a whole-brain neural mass model [43](#). We used the default model of the `neurolib` python library (“ALNModel”), which is a mean-field approximation of adaptive exponential integrate-and-fire neurons. This model can generate simulated mean firing rates in 80 brain areas based on connectivity and delay matrices determined with diffusion tensor imaging (DTI). We used 5 min of “resting state” activity (no added stimulus, simulated at 0.1ms resolution, subsequently downsampled to 100Hz). The true connectivity matrix from DTI (**Fig. 2A**) appears to be similar to the effect size estimate R for the recurrent connections A in the VARX model with no input (**Fig. 2B**). Following [44](#) we compare the two as a scatter plot (**Fig. 2C**) and observed a Spearman correlation of 0.69. For comparison, we also used the sparse-inverse covariance method to recover structural connectivity from functional connectivity. This method is more sensitive than others in detecting network connections [45](#) and uses the graphical lasso algorithm [46](#). The resulting connectivity estimate (**Fig. 2D**) only achieves a Spearman correlation of 0.52. We note that the structural connectivity determined with DTI is largely symmetric. When enhancing the asymmetry the VARX model is not as accurate, but correctly recovers the direction of the asymmetry (Fig. S1).

Intracranial EEG recordings and stimulus features

We analyzed intracranial EEG and simultaneous eye-tracking data recorded from patients ($N=21$, mean age 37.81 years, age range 19-58 years, 9 female, Table S1) during rest and while they watched various video clips. Three patients underwent two implantations and recordings at different times resulting in a total of 24 recording sessions with a total of 4,962 recording channels. The video clips included animations with speech (‘Despicable Me’, two different clips, 10 min each, in English and Hungarian), an animated short film with a mostly visual narrative and music, shown twice (‘The Present’, 4.3 min), and three clips of documentaries of macaques (‘Monkey’, 5 min each, without sound) [48](#). In addition to the clips from the previous analysis, we included a movie clip of abstract animations (‘Inscapes’, 10 min) [49](#), and an eyes-open resting state with maintained fixation (‘Resting state’, 5 min). In total, we recorded up to 59.3 minutes of data for each patient (Table S1). Two patients did not complete both movie watching and resting state (Pat_5 & Pat_16) and were not included in the analysis that compares the two conditions.

Neural signals were preprocessed as previously described to reduce noise [48](#). We re-reference signals in a bipolar montage to ensure analysis of local activity. We analyze local field potentials (LFPs) and broadband high-frequency activity (BHA) power. BHA is the power of the signal bandpass filtered between 70-150Hz. We perform analysis on both signals after downsampling to 60Hz. Example traces of $y(t)$ for LFP and BHA are shown in **Fig. 1B&C**.

We extract three features of the movies that serve as external inputs for the VARX model: fixation onset, film cuts and sound envelope (**Fig. 3G**). Fixation onset and film cuts are represented in $x(t)$ as pulse trains with pulses occurring at the time of these events [48](#). Sound envelope is computed as the absolute value of the Hilbert transform of the sound from the movie files and varies continuously. The envelope is downsampled to 60 Hz. All videos and resting state include fixations. The video ‘Inscapes’ and resting state do not include film cuts as external input. The ‘Monkey’ video clips and resting state do not include the sound envelope as input features, but do include fixation onsets. When a feature is not available it is replaced with features from a different recording. Therefore, the statistics of the feature are consistent, but not aligned to the neural recording. When comparing models with different features we always keep the number of

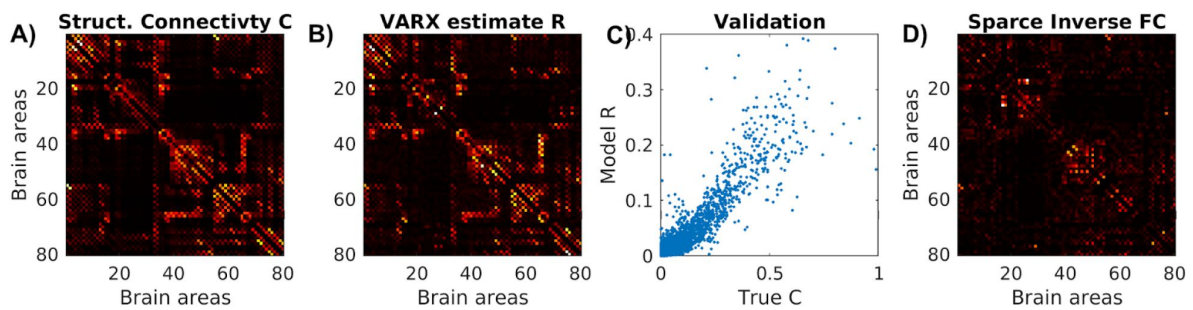


Figure 2

Connectivity of stimulated neural mass model for the whole brain, and estimated VARX model.

A) True structural connectivity used to simulate neural activity using a neural mass model with the neurolib python toolbox. Connectivity is based on diffusion tensor imaging data between 80 brain areas (called Cmat in neurolib). Here showing the square root of the “Cmat” matrix for better visibility of small connectivity values. B) Effect size estimate R for the A matrix of the VARX model on the simulated data. C) Comparison of true and VARX estimate of connectivity. D) Absolute value of the sparse-inverse functional connectivity (estimated using graphical lasso⁴⁷).

input variables consistent between models to avoid a bias by the number of free parameters of the model. Features that are not considered in the analysis are shuffled in time by a circular shift by half the duration of the signals.

The VARX models were fitted to data with the matlab version of the code [31](#). For all analyses we use filters of 600 ms length for inputs ($n_b=36$ samples for VARX models, $L=36$ samples for mTRF models). Delays for connections between channels are set to 100ms ($n_a=6$ samples) for both LFP and BHA signals. Increasing the number of delays n_a , increases estimated effect size R , however, larger values lead to overfitting, i.e. less significant connections (Fig. S1). Values around $n_a=6$ samples achieve a balance between goodness of fit and overfitting (Fig. S2). The regularization parameter was set to $\lambda=0.3$.

Connectivity plots are created with Nilearn's `plot_connectome()` function (Fig. 4) [50](#). We plot only significant connections ($p<0.001$). Surface plots of T1w/T2w ratios and directionality of connections are created using the field-echos repository [51](#), [52](#). T1w/T2w maps [53](#) are obtained from the neuromaps repository [54](#), [55](#), and transformed to the freesurfer surface using the `fslr_to_fsaverage()` function [56](#), [57](#).

The length of responses for Fig. 5 is computed as the 'peak widths' argument of Matlab's `findpeaks()` function. Power is computed as the average of the instantaneous power, i.e. the square of the weight at each delay of the filters.

Data and code availability

The raw data reported in this study cannot be deposited in a public repository because of patient privacy concerns. To request access, contact The Feinstein Institutes for Medical Research, through Dr. Stephan Bickel. In addition, processed datasets derived from these data have been deposited at <https://doi.org/10.17605/OSF.IO/V25T> and are publicly available as of the date of publication.

All original code has been deposited at https://github.com/MaxNentwich/varx_demo.

Results

Extrinsic input leads to spurious intrinsic connectivity

To determine the effect of the extrinsic inputs on connectivity estimates we either fit a VARX model or a VAR model (i.e. a VARX model with no external input). We analyze LFP data on all available recordings, movies and resting state for all $N=24$ recording sessions. As extrinsic inputs we included film cuts, fixation onset, and sound envelope. VAR models contain the same external inputs as the VARX model, but the time alignment is disrupted by a circular shuffle. This keeps the number of parameters in different models constant and ensures the inputs have the same covariance structure. We found a similar connectivity structure for the estimated VAR and VARX models (Fig. 3A and 3B). However, they vary systematically in the number of significant recurrent connections A (those with $p<0.001$, Fig. 3D), which drops when adding inputs (median $=-8.7*10^{-4}$, $p<0.001$, $N=24$, Wilcoxon). The effect sizes R also significantly decreases in the VARX model (Fig. 3E, median $=-1.9*10^{-5}$, $p<0.001$, $N=24$, Wilcoxon). Therefore, accounting for the external input removes spurious "connections". We also analyzed how much each of these inputs contributed to this effect (Fig. 3F). Out of the three input features considered, models including fixations and cuts decrease effect size more than models with sound envelope (fixations vs. sound, median $\Delta R=-1.0*10^{-5}$, $p<0.001$, $N=24$; cuts vs. sound: median $\Delta R=-3.8*10^{-6}$, $p<0.001$, $N=24$; Wilcoxon, uncorrected). The model including the combination of all three features has a smaller effect size R for A than models with any individual input feature (all vs. fixations: median $\Delta R=-6.5*10^{-6}$, $p<0.001$, $N=24$; all vs. cuts: median $\Delta R=-1.2*10^{-5}$, $p<0.001$, $N=24$; all vs. sound: median $\Delta R=-1.9*10^{-5}$,

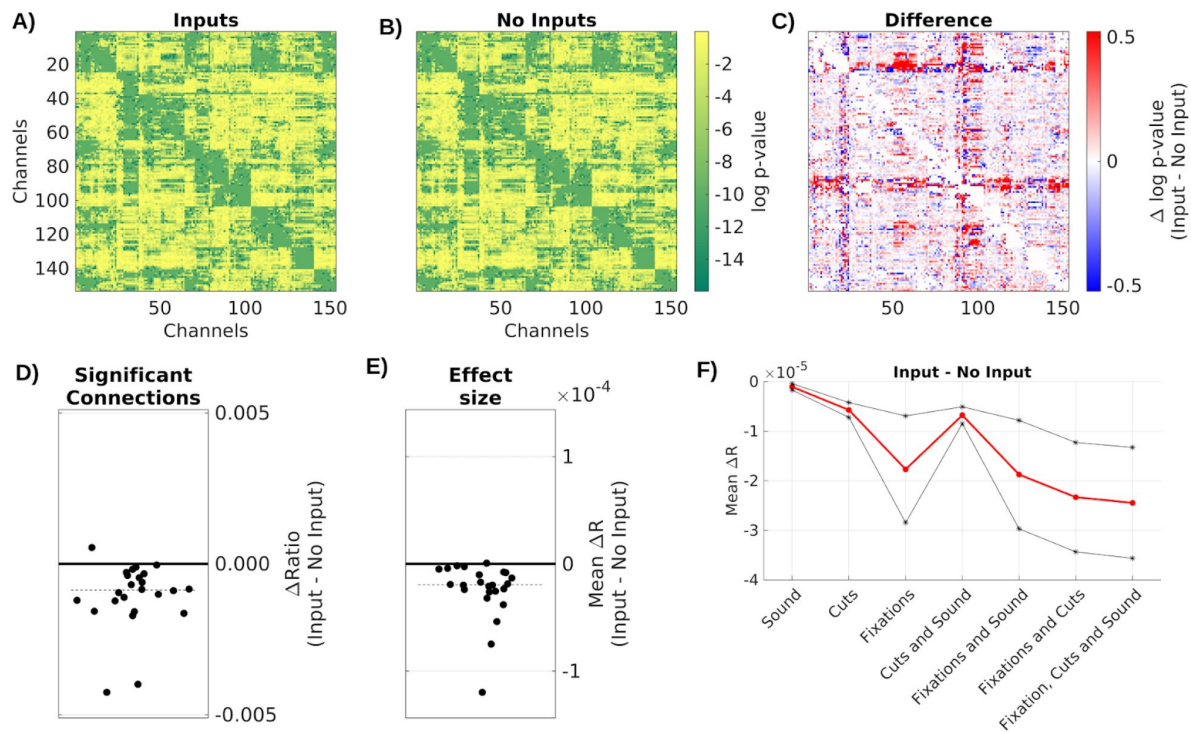


Figure 3

Spurious intrinsic connectivity in A is removed when modeling the effect of exogenous input with B.

Comparison of VARX model with and without inputs. A) p -values for each connection in A for VARX model with inputs on one subject (Pat_1); B) for VARX model without inputs; C) difference. Both models are fit to the same data. D) Difference of fraction of significant recurrent connections between VARX models with and without inputs. E) Mean difference in R over all electrodes between VARX models with and without inputs. Each point is a subject. Dashed line is the median across subjects. F) Difference between the VARX models with different input combinations and the VARX model without inputs. Red line shows mean across patients, black lines the 95% confidence interval. Negative values indicate a decrease in connectivity strength when exogenous input is accounted for.

Figure 4

Recurrent connectivity A during movies does not detectably differ from rest.

Effect size R for each connection in A. A) VARX model of 5 minutes of LFP recordings during movie watching, with sound envelope, fixation onsets and film cuts as input features. B) VARX model during resting fixation with fixation onset as input feature. C) Difference in the number of significant connections ($p < .0001$) between movie and rest. D) Difference in mean effect size across all channels between movie and rest. Dots represent subjects, dashed line the median across subjects. Axial view of significant connections in E) the movie task, F) resting state, and G) the difference between movies and resting state. Dots show the location of contacts in MNI space. Lines show significant connections between contacts. For plotting purposes connections in the upper triangle are plotted and asymmetries ignored. Only channels with p -values < 0.001 in both conditions are plotted.

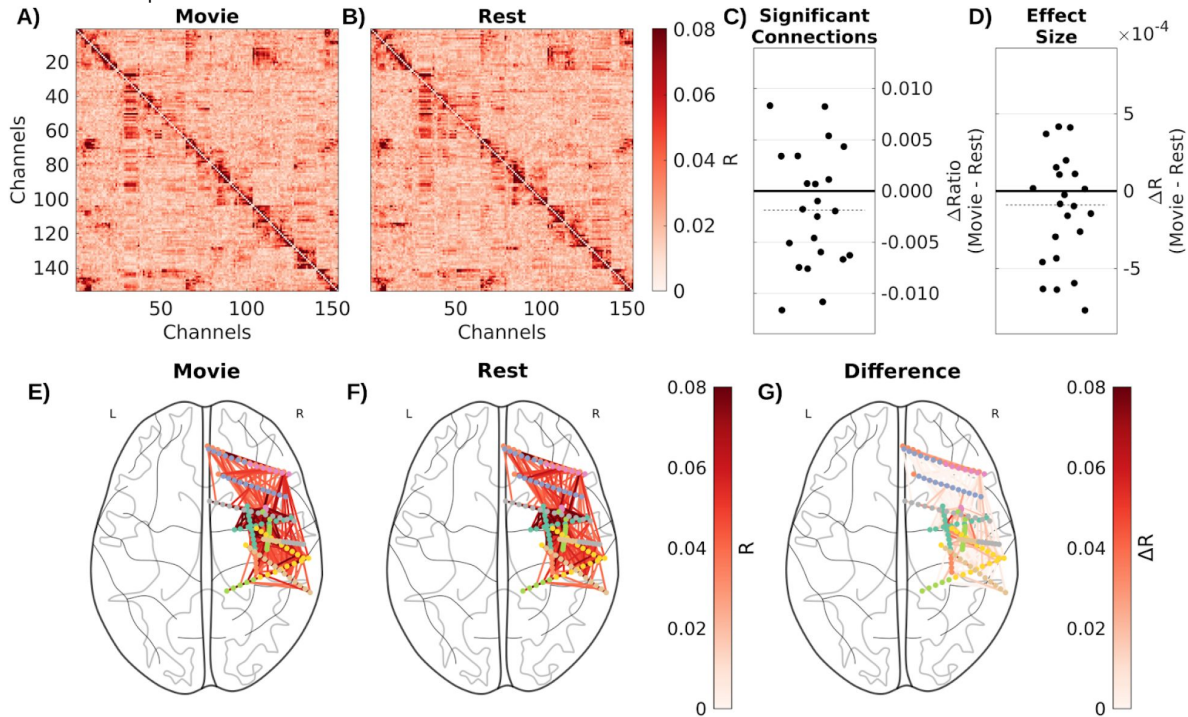
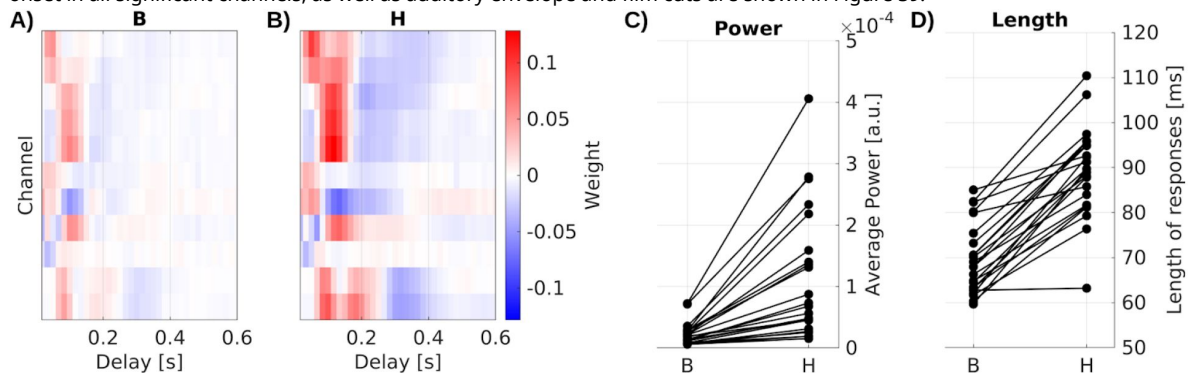


Figure 5

Impulse response models.

A) Immediate responses B to fixation onset are weaker and shorter than B) the overall system response H. Significant responses of select channels in for one example patient. C) Power and D) mean length of responses in significant channels for all patients. Each line is a patient. Channels with the strongest responses are shown in panels A&B. Responses to fixation onset in all significant channels, as well as auditory envelope and film cuts are shown in Figure S9.



$p < .0001$, $N = 24$; Wilcoxon, uncorrected). Thus, adding more input features further reduces the strength of intrinsic “connections”. These results are also reflected in the analysis of BHA signals (Fig. S3).

Recurrent connectivity unchanged during movies and rest

Next we compared intrinsic “connectivity” between movie watching and rest (Fig. 4A-D). In the rest condition subjects have a fixation cross on a gray background. This obviously reduces the size and number of saccades as compared to movie watching, but does not abolish them (Fig. S4). We therefore use a VARX model including fixation onset as extrinsic variable in both cases. Movies include film cuts and the sound envelope as external inputs. To control for the number of free parameters, we include copies of the film cut and sound envelope features from the movies to the resting state model. Remarkably, the number of significant recurrent connections in A were not detectably different between movie watching and rest (Fig. 4C, median = -0.0019, $p = 0.19$, $N = 22$, Wilcoxon), as is the effect size (Fig. 4D, median = -9×10^{-5} , $p = 0.14$, $N = 22$, Wilcoxon). One caveat to this conclusion is that the signal we analyzed was only 5 minutes long for the movie and rest conditions, and longer records may have revealed small differences. However, even on 5 minutes of data we observe a decrease in R values when including external inputs (Fig. S5). Connectivity of BHA between movie and rest does also not differ significantly (Fig. S6). Using different segments of movies, in some cases we find a small reduction of significant connections in movie watching compared to resting state conditions (Fig. S7). However, overall, differences in the intrinsic connectivity between movie and rest, if they exist, are less systematic than the effect of the stimulus.

Recurrent dynamic enhances and prolongs stimulus responses

We also compared the immediate exogenous effect B with the total system response H, which includes the additional effect of the recurrent dynamic A. We estimate B with the VARX model (Fig. 5A) on data during video watching, and estimate the total response H directly using temporal response functions (Fig. 5B). Both models include fixation onset, film cuts and sound envelope as external inputs. We compare the power and length of filters from both models (Fig. 5C-D). We compare responses in channels with significant effects of B (FDR correction, $\alpha = 0.05$). We see that the total response fixation onset is significantly stronger (Fig. 5C, median $\Delta = -5.4 \times 10^{-5}$, $p < .0001$, $N = 23$, Wilcoxon) and longer than the immediate effect B (Fig. 5D, median $\Delta = -21.72$ ms, $p < .0001$, $N = 23$, Wilcoxon). The same effect is observed for other input features and for BHA responses (Fig. S8). This suggests that the total response of the brain to these external inputs is dominated by the recurrent dynamic of the brain.

Results are similar for VARX models of BHA and LFP

We repeated the same analyses of Figures 3-5 with broadband high frequency activity (BHA). While LFP are thought to capture dendritic currents, BHA is correlated with neuronal firing rates in the vicinity of an electrode. Generally we find a more sparse recurrent connectivity for BHA as compared to LFP (compare Fig. 3&4 with Fig. S3&S6). Perhaps this is expected, given that LFP covers a broader frequency range. Regardless of this overall difference, we find similar results when analyzing BHA with the VARX model. Namely, taking the extrinsic input into account removed stimulus-induced intrinsic “connections” (Fig. S3); the resulting model of the recurrent dynamic is indistinguishable between watching movies and rest (Fig. S6); and responses to the stimulus are stronger and more prolonged when separately modeling the effect of recurrent connectivity (Fig. S8). In the Discussion section we will argue that some of these results are expected in general when decomposing the total system response into extrinsic and intrinsic effects. What we did not necessarily expect is that the intrinsic dynamics is similar during movies and rest for both LFP and BHA.

Intrinsic “noise” in BHA is reduced by external stimulus

So far we have discussed the mean response captured by B and the recurrent activity mediated by A. We now want to analyze whether the external input modulates the variability of the internal dynamic. As a metric of internal variability we measured the power of the intrinsic innovation process $e(t)$. For the LFP signal we see a drop in power during movies as compared to rest, for both the original signal $y(t)$ (Fig. S10A) and the model’s innovation process $e(t)$ (Fig. S10B). Notable is the stronger oscillatory activity during rest (Fig. S10A). In this example we see a drop in power in the theta/alpha band (5-11 Hz) during movie watching across all electrodes (Fig. S10A, dotted lines). We observe similar narrow-band drop in power in most patients, albeit at different frequencies (not shown). When analyzing BHA, we find no difference in power of the innovation process between movie and rest, but we do find a drop in power relative to the overall BHA signals for some channels (Fig. 6B). These channels seem to coincide with channels that responded to the external stimuli, i.e. channels with a significant effect in B (Fig. 6A). If we take for each subject the median relative power for responsive channels (median among those with $p < 0.0001$), then we find that relative power drops for nearly all subjects (Fig 6D, Wilcoxon rank sum test, $p = 2.6e-06$, $N = 21$). The motivation for analyzing only responsive channels comes from a simple gain adaptation (Fig. S11). Gain adaptation keeps the power of $y(t)$ constant, so that the extra power injected by the stimulus implicitly reduces the relative power of the innovation process. This effect is specific to channels receiving external input (Fig. S11D) and absent in a linear system without gain adaptation (Fig. S11C). To demonstrate that this simple gain adaptation can explain the noise quenching in the neural data, we simulated data with the gain adaptation model (Fig. 6C) using parameters estimated for the example subject of Fig. 6A/B.

Direction of connectivity differs with cortical hierarchy

Finally, we measured the directionality of the recurrent connections in the LFPs by analyzing the structure of the resulting matrices R of all subjects. Columns in R represent outgoing connections, while rows are incoming connections. Therefore, the difference of $R - R^T$ (Fig. 7A) averaged along a column has positive values if a node has overall stronger outgoing connections, and negative values if it has stronger incoming connections. We measured this directionality for each channel across all subjects and averaged also across channels within parcels of the Desikan-Killiany atlas ($N = 35$ regions of interest, Fig. 7B). We expected this to co-vary with “cortical hierarchy”. To test this, we compared this asymmetry metric with the T1w/T2w ratio, which captures gray matter myelination and is used as an indirect measure of cortical hierarchy (Fig. 7B). We also average T1w/T2w ratio in the same parcels of the Desikan-Killiany atlas (Fig. 7B). Cortical areas showing more outgoing connections ($R - R^T > 0$) have lower T1w/T2w ratio, which are located higher on the cortical hierarchy (Pearson’s $r = 0.39$, $p = 0.023$, Fig. 7C). BHA analysis shows the same trend (Fig. S12).

Discussion

Our results suggest that intrinsic dynamics are not substantially altered during watching movies as compared to rest. Instead, the external stimulus reverberates in the recurrent network with the same dynamic as during rest. The duration and magnitude of response is in large part a result of this recurrent dynamic.

Response to extrinsic input versus intrinsic dynamics

Previous literature does often not distinguish between intrinsic connectivity and extrinsic effects. As a result, similarities and differences between rest and stimulus conditions reported previously, do not draw a firm conclusion as to whether “functional connectivity” is preserved, e.g. (Fig. 12, 16).

Figure 6

For BHA, relative power of innovation vs signal drops during movies as compared to rest in responsive channels.

A) Effect size R for extrinsic effect B in all channels for 3 input features (scene cuts, fixation onset, sound envelope). In this example 15 electrodes had significant responses to one of the three inputs (Bonferroni corrected at $p < 0.01$). B) Change in relative power of innovation (dB(innovation power / signal power), then subtracting movie - rest). C) Change in relative power of innovation in a simulation of a VARX model with gain adaptation. Here we are using the A and B filters that were estimated on BHA on the example from panel A and B. D) Median of power ratio change across all subjects, contrasting responsive vs non-responsive channels.

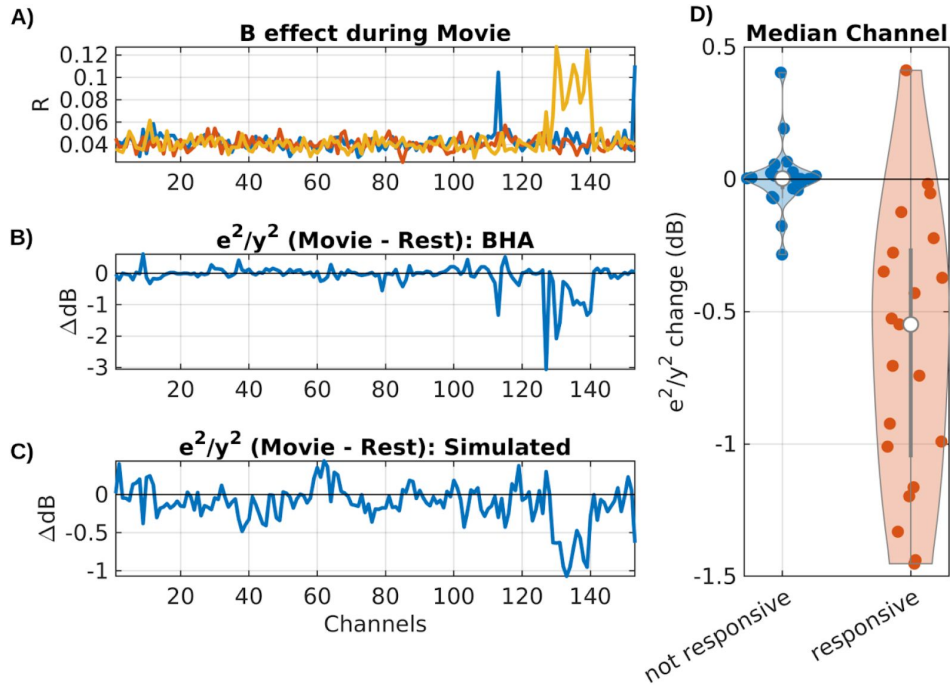
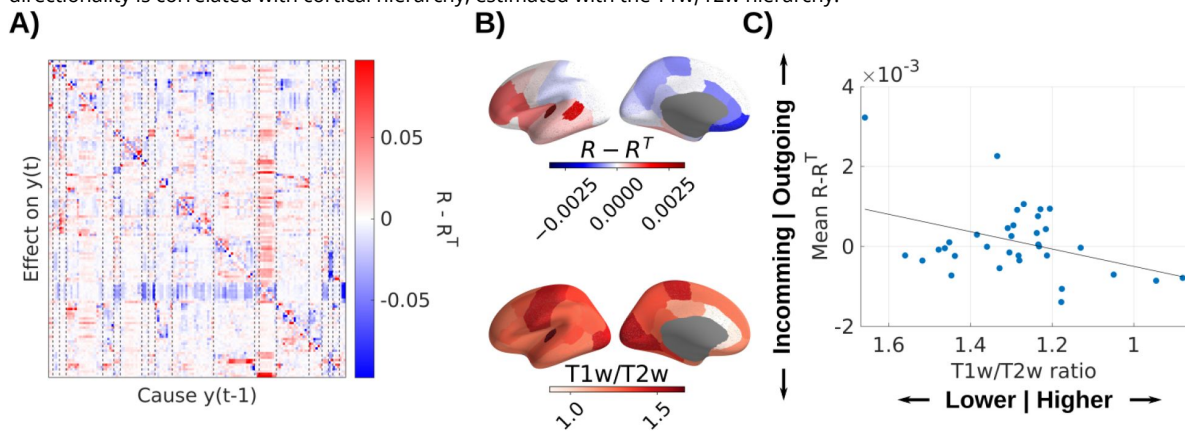


Figure 7

Recurrent connectivity of LFP is directed from sensory to higher-order areas.

A) Difference of $s - R^T$ showing asymmetric directed effects. Dashed lines indicate regions of interest in the Desikan-Killiany atlas. B) Mean directionality across patients and T1w/T2w ratio are averaged in parcels of the Desikan-Killiany atlas. C) Mean directionality is correlated with cortical hierarchy, estimated with the T1w/T2w hierarchy.



By systematically factoring out the effect of the external input we conclude here that the intrinsic dynamic is unaltered. If one fails to factor out the effect of the stimulus, one may mistake the stimulus-induced correlations for changes in “functional connectivity”.

In this work we focused on “passive” tasks, i.e. resting with gaze on a fixation point, versus watching movies without any associated tasks. We did not analyze data during an active task requiring behavioral responses. The literature on active tasks emphasizes “state change” in functional connectivity. ¹⁴,²⁰,⁶⁰. Efforts to factor out task-evoked activity when computing functional connectivity concord with our conclusions that connectivity is inflated by a task ¹⁷. Nevertheless, we hesitate extrapolating our findings to active tasks, as we have not analyzed such data.

Conventional “encoding” models, such as temporal response functions, capture the total response H of the brain to an external stimulus. Here we factored this into a moving average filter B , followed by an autoregressive filter A . The important observation is that this intrinsic dynamic governed by A does not change during stimulus processing. Arguably then, the role of the initial responses B is to shape the input to be processed by the existing intrinsic dynamic. This interpretation is consistent with the view of “the brain from the inside out” advocated by György Buzsáki ⁶¹. In this view, learning of a stimulus representation consists in learning a mapping of the external stimulus to an existing intrinsic dynamic of the brain.

Similar findings for LFP and BHA

We found a more sparse recurrent connectivity for BHA as compared to LFP. This may be expected because correlations in lower frequencies (that dominate LFPs) reaches over longer distances compared to correlations in higher frequencies (e.g. Muller et al., 2016). BHA has been linked to a mixture of neuronal firing and dendritic currents ⁶², in contrast to LFP, which is thought to originate from widespread dendritic currents. Despite the observed differences in sparsity, for both LFP and BHA we found that modeling the recurrent dynamic removed spurious intrinsic connections. Removal of spurious effects when controlling for a common cause is a generic finding in multivariate statistical models. We also found for both LFP and BHA that the duration and strength of stimulus responses can be largely attributed to the recurrent dynamic. Arguably, this is a generic feature of an autoregressive model, as it more readily captures longer impulse responses. However, the extrinsic filters B in principle have an advantage as they can be fit to each stimulus and brain location. In contrast, the recurrent filters A are constrained by having to capture a shared dynamic for all stimulus dimensions. Thus, the predominance of the recurrent dynamic in the total system response is not a trivial result of the factorization into intrinsic and extrinsic effects. Finally, we did not necessarily expect that the intrinsic connectivity is preserved between movie and rest in both LFP and BHA. This consistency may be due to a variety of processes that are constant across conditions, such as internal thought, body and eye movements. Active sensing through eye movements, for example, influences activity in a global network ⁶³,⁶⁴, and likely accounts for part of the common source of correlations across conditions.

Stimulus-induced reduction of noise in the intrinsic activity

One difference we did find between LFP and BHA is the intrinsic innovation process, i.e. the internal sources of variability or “noise”. For both BHA and LFP we saw a drop in the magnitude of signal fluctuations during the movie watching condition. For the BHA but not the LFP, this was explained as a drop in intrinsic noise. Specifically, for BHA there was less relative power in the intrinsic “noise” for channels that are responsive to the stimulus. This is consistent with the notion that response variability is due to variability of intrinsic activity ²², which is found to decrease across the brain with the onset of an external stimulus ⁶⁵. This type of noise quenching has been associated with increased attention ⁶⁶ and improved visual discrimination performance ⁶⁷. The effect we found here can be explained by a VARX model with the addition of a divisive gain

adaptation mechanism that keeps the total power of brain activity constant. When the input injects additional power, this nonlinear gain adaptation implicitly reduces the contribution of the intrinsic noise to the total power.

We also observed an overall drop in LFP power during movie watching. This phenomenon was strongest in oscillatory bands, with frequencies in theta to beta band differing across subjects. In scalp EEG, noise quenching is associated with a similar overall drop in power with the stimulus [66](#). This quenching of neural variability was also found to reduce correlation between brain areas for fMRI and neural spiking [26](#). Both fMRI and neural spiking correlated with BHA [68](#). This is at odds with our finding that intrinsic connectivity in BHA does not change significantly between movie and rest. However, we can not rule out such differences on longer recordings.

Stimulus features

During the movie and rest periods, we utilized fixation onset to capture activity that is time-locked to visual processing because subjects move their eyes even during rest. We also incorporated the sound envelope, a prominent feature known for capturing the dominant audio-induced variance in scalp EEG [33](#). In addition, we included film cuts as features, as we had previously demonstrated that they dominate the response in the BHA across the brain [48](#). While other basic visual features such as overall optic flow or fixations on faces elicited responses in the BHA, their contribution was relatively smaller. The analysis is not limited to these few features, and future research should explore which stimulus features capture variance in the data and how they affect the apparent intrinsic connectivity. There is a substantial body of literature on encoding models of semantic features, where nonlinear features of a continuous natural stimulus are extracted and then linearly regressed against fMRI [69](#), [70](#) or EEG [71](#). This work can be directly replicated with the VARX model which further models the intrinsic connectivity.

Alternative approaches

The traditional VAR model has been used extensively in neuroscience to establish directed “Granger causal” connections [41](#). This approach has been very fruitful and found numerous extensions, e.g. [10](#), [11](#). However, these model implementations do not specifically account for an external input.

A few methods have attempted to model the effect of varying task conditions on functional connectivity, mostly in the analysis of fMRI. One approach is to first model the task-evoked responses, equivalent to estimating \mathbf{B} alone, and then compute the conventional “functional connectivity”, i.e. the correlation matrix, on the residuals $e(t)$ [72](#). Others suggested to estimate \mathbf{B} in multiple time windows and then estimate a “task related functional connectivity” by correlating the multiple \mathbf{B} over time windows [73](#). It is not clear that these ad-hoc methods systematically separate intrinsic from extrinsic factors.

A more principled modeling approach is “dynamic causal modeling” (DCM) [19](#) and extensions thereof [74](#). Similar to the VARX model, DCM includes intrinsic and extrinsic effects \mathbf{A} and \mathbf{B} . However, the modeling is limited to first-order dynamics (i.e. $n_a = n_a = 1$). Instead, the DCM includes a multiplicative interaction of extrinsic input $x(t)$ on the connectivity \mathbf{A} , which does not exist in the VARX model. This interaction has been used to explicitly model a change in intrinsic connectivity with task conditions. Here we found that this may not be necessary for intracranial EEG. A practical advantage of the VARX model is the assumption that the neural activity is directly observed. Instead, many existing models assume an error in the observations, which triggers computationally intensive estimation algorithms, typically the expectation maximization algorithm. The same is true for the “output error” model in linear systems theory [29](#). As a result, these models are often limited to small networks (The original DCM proposed for fMRI included an added complication of modeling the hemodynamic response, which amounts to adding a temporal

filter to each output node and prior to adding observation noise.) to test specific alternative hypotheses ⁴². In contrast, here we have analyzed 100-200 channels per subject across the brain, and have drawn more general conclusions about whole-brain activity.

Caveats

The lack of a significant difference in recurrent connectivity between stimulus and rest should be interpreted with care. As usual, lack of evidence is not evidence for the lack of an effect. We saw no change in the number of recurrent connections between movie and rest, either for the LFPs or BHA activity. However, in individual movie segments small differences were observed (Fig. S7). It is possible that regressing out a richer stimulus characterization would have removed additional stimulus-induced correlation, only enhancing this small difference between movie and rest. We were also limited to 5 minutes of data in the direct comparison of movie and resting state data. Longer recordings might further enhance differences. Higher recurrent connectivity in the LFP during rest would be consistent with the more synchronized state we saw in rest, as reflected by larger oscillatory activity.

We find a correlation of DTI structural connectivity used in a model with a VARX estimate of 0.70. That is considered a relatively large value compared to other studies that attempt to recover DTI connectivity from the correlation structure of fMRI activity ⁴⁴. A Caveat is that this was done on a biophysical model of firing rate, not fMRI, and we have not explored the parameters of the model that might affect the results.

We used fixation onsets as external input, but it should be noted that they are tightly correlated in time with saccade onsets (there is only about a 30 ms jitter between the two, depending on saccade amplitude). While saccades are driven by visual movement, they are generated by the brain itself and arguably could also be seen as intrinsic. The same is true for all motor behaviors, most of which cause a corresponding sensory response, similar to the visual response following a saccade. Including them as external input is a modeling choice we have made here, but it is important to acknowledge that fixation onsets can therefore have “acausal” components ⁴⁸. By “acausal” we mean a fixation-locked response that precedes the fixation onset and is due to the neural activity leading up to the saccade and subsequent fixation. Such acausal responses can be captured by the VARX Granger formalism by delaying the input relative to the neural activity, which we have not done here.

The correlation between the average incoming and outgoing connections and cortical hierarchy (Fig. 7) is not significant when normalizing for the number of electrodes in each region of interest. Regions in the temporal lobe with a large number of electrodes might drive this correlation. A more fine grained analysis in these regions could be the goal of future analysis.

Conclusion

We analyzed whole-brain intracranial recordings in human subjects at rest and while they watched videos. We used a model that separates intrinsic dynamics from extrinsic effects. We found that the recurrent dynamic observed during rest is largely unaltered when watching movies. Instead, the brain’s response to the audiovisual stimuli appears to be substantially shaped by its endogenous dynamic. The reduction in intrinsic variance observed during an extrinsic stimulus may be the result of neuronal gain adaptation.

Acknowledgements

We would like to thank Chris Honey for advice on the model validation with simulations and related references. We like to thank Behtash Babadi for help on the development of the Granger formalism for the VARX model. This work was supported in part by the NIH through grants P50 MH109429 and R01DC019979.

Additional information

Author contributions

Conceptualization, L.C.P. and M.N.; Methodology, L.C.P.; Software, L.C.P. and M.N.; Formal Analysis: M.N and L.C.P.; Investigation, M.N. and M.L.; Resources, S.B.; Writing – Original Draft, L.C.P. and M.N.; Writing – Review & Editing, L.C.P., M.N., M.L., C.E.S., S.B.; Funding Acquisition, L.C.P., C.E.S. and S.B.; Visualization, M.N.; Supervision, L.C.P., C.E.S., S.B.

Additional files

Supplemental information [↗](#)

References

1. Felleman D.J., Van Essen D.C. 1991) **Distributed Hierarchical Processing in the Primate Cerebral Cortex** *Cereb. Cortex* **1**:1–47 <https://doi.org/10.1093/cercor/1.1.1-a>
2. Friston K.J., Holmes A.P., Poline J.-B., Grasby P.J., Williams S.C.R., Frackowiak R.S.J., Turner R. 1995) **Analysis of fMRI Time-Series Revisited** *NeuroImage* **2**:45–53 <https://doi.org/10.1006/nimg.1995.1007>
3. Lalor E.C., Foxe J.J. 2010) **Neural responses to uninterrupted natural speech can be extracted with precise temporal resolution** *Eur. J. Neurosci* **31**:189–193 <https://doi.org/10.1111/j.1460-9568.2009.07055.x>
4. Greicius M.D., Krasnow B., Reiss A.L., Menon V. 2003) **Functional connectivity in the resting brain: A network analysis of the default mode hypothesis** *Proc. Natl. Acad. Sci* **100**:253–258 <https://doi.org/10.1073/pnas.0135058100>
5. Varela F., Lachaux J.-P., Rodriguez E., Martinerie J. 2001) **The brainweb: Phase synchronization and large-scale integration** *Nat. Rev. Neurosci* **2**:229–239 <https://doi.org/10.1038/35067550>
6. Friston K., Moran R., Seth A.K. 2013) **Analysing connectivity with Granger causality and dynamic causal modelling** *Curr. Opin. Neurobiol* **23**:172–178 <https://doi.org/10.1016/j.conb.2012.11.010>
7. Haufe S., Nikulin V.V., Müller K.-R., Nolte G. 2013) **A critical assessment of connectivity measures for EEG data: A simulation study** *NeuroImage* **64**:120–133 <https://doi.org/10.1016/j.neuroimage.2012.09.036>
8. Pellegrini F., Delorme A., Nikulin V., Haufe S. 2023) **Identifying good practices for detecting inter-regional linear functional connectivity from EEG** *NeuroImage* **277**:120218 <https://doi.org/10.1016/j.neuroimage.2023.120218>
9. Seth A.K., Barrett A.B., Barnett L. 2015) **Granger Causality Analysis in Neuroscience and Neuroimaging** *J. Neurosci* **35**:3293–3297 <https://doi.org/10.1523/JNEUROSCI.4399-14.2015>
10. Sheikhattar A., Miran S., Liu J., Fritz J.B., Shamma S.A., Kanold P.O., Babadi B. 2018) **Extracting neuronal functional network dynamics via adaptive Granger causality analysis** *Proc. Natl. Acad. Sci* **115**:E3869–E3878 <https://doi.org/10.1073/pnas.1718154115>
11. Soleimani B., Das P., Dushyanthi Karunathilake I.M., Kuchinsky S.E., Simon J.Z., Babadi B. 2022) **NLGC: Network localized Granger causality with application to MEG directional functional connectivity analysis** *NeuroImage* **260**:119496 <https://doi.org/10.1016/j.neuroimage.2022.119496>
12. Betti V., Della Penna S., de Pasquale F., Mantini D., Marzetti L., Romani G.L., Corbetta M. 2013) **Natural Scenes Viewing Alters the Dynamics of Functional Connectivity in the Human Brain** *Neuron* **79**:782–797 <https://doi.org/10.1016/j.neuron.2013.06.022>

13. Geerligs L., Rubinov M., Henson R.N. 2015) **State and Trait Components of Functional Connectivity: Individual Differences Vary with Mental State** *J. Neurosci* **35**:13949–13961 <https://doi.org/10.1523/JNEUROSCI.1324-15.2015>
14. Mennes M., Kelly C., Colcombe S., Castellanos F.X., Milham M.P. 2013) **The Extrinsic and Intrinsic Functional Architectures of the Human Brain Are Not Equivalent** *Cereb. Cortex* **23**:223–229 <https://doi.org/10.1093/cercor/bhs010>
15. Vanderwal T., Eilbott J., Finn E.S., Craddock R.C., Turnbull A., Castellanos F.X. 2017) **Individual differences in functional connectivity during naturalistic viewing conditions** *NeuroImage* **157**:521–530 <https://doi.org/10.1016/j.neuroimage.2017.06.027>
16. Demirtaş M., Ponce-Alvarez A., Gilson M., Hagmann P., Mantini D., Betti V., Romani G.L., Friston K., Corbetta M., Deco G. 2019) **Distinct modes of functional connectivity induced by movie-watching** *NeuroImage* **184**:335–348 <https://doi.org/10.1016/j.neuroimage.2018.09.042>
17. Cole M.W., Ito T., Schultz D., Mill R., Chen R., Cocuzza C. 2019) **Task activations produce spurious but systematic inflation of task functional connectivity estimates** *NeuroImage* **189**:1–18 <https://doi.org/10.1016/j.neuroimage.2018.12.054>
18. Pearl J. 2013) **Linear Models: A Useful “Microscope” for Causal Analysis** *J. Causal Inference* **1**:155–170 <https://doi.org/10.1515/jci-2013-0003>
19. Friston K.J., Harrison L., Penny W. 2003) **Dynamic causal modelling** *NeuroImage* **19**:1273–1302 [https://doi.org/10.1016/S1053-8119\(03\)00202-7](https://doi.org/10.1016/S1053-8119(03)00202-7)
20. Gonzalez-Castillo J., Bandettini P.A. 2018) **Task-based dynamic functional connectivity: Recent findings and open questions** *NeuroImage* **180**:526–533 <https://doi.org/10.1016/j.neuroimage.2017.08.006>
21. Fox M.D., Snyder A.Z., Zacks J.M., Raichle M.E. 2006) **Coherent spontaneous activity accounts for trial-to-trial variability in human evoked brain responses** *Nat. Neurosci* **9**:23–25 <https://doi.org/10.1038/nn1616>
22. Arieli A., Sterkin A., Grinvald A., Aertsen A. 1996) **Dynamics of Ongoing Activity: Explanation of the Large Variability in Evoked Cortical Responses** *Science* **273**:1868–1871 <https://doi.org/10.1126/science.273.5283.1868>
23. Buzsaki G. 2006) **Rhythms of the Brain** Oxford University Press
24. Fiser J., Chiu C., Weliky M. 2004) **Small modulation of ongoing cortical dynamics by sensory input during natural vision** *Nature* **431**:573–578 <https://doi.org/10.1038/nature02907>
25. Gray C.M., König P., Engel A.K., Singer W. 1989) **Oscillatory responses in cat visual cortex exhibit inter-columnar synchronization which reflects global stimulus properties** *Nature* **338**:334–337 <https://doi.org/10.1038/338334a0>
26. Ito T., Brincat S.L., Siegel M., Mill R.D., He B.J., Miller E.K., Rotstein H.G., Cole M.W. 2020) **Task-evoked activity quenches neural correlations and variability across cortical areas** *PLOS Comput. Biol* **16**:e1007983 <https://doi.org/10.1371/journal.pcbi.1007983>
27. Nauhaus I., Busse L., Carandini M., Ringach D.L. 2009) **Stimulus contrast modulates functional connectivity in visual cortex** *Nat. Neurosci* **12**:70–76 <https://doi.org/10.1038/nn.2232>

28. Roelfsema P.R., Engel A.K., König P., Singer W. 1997) **Visuomotor integration is associated with zero time-lag synchronization among cortical areas** *Nature* **385**:157–161 <https://doi.org/10.1038/385157a0>
29. Ljung L. 1999) **System Identification: Theory for the User**
30. Hamilton J.D. 2020) **Time Series Analysis** Princeton University Press
31. Parra L.C., Silvan A., Nentwich M., Madsen J., Babadi B. 2024) **VARX Granger Analysis: Modeling, Inference, and Applications** *arXiv*
32. Naselaris T., Kay K.N., Nishimoto S., Gallant J.L. 2011) **Encoding and decoding in fMRI** *NeuroImage* **56**:400–410 <https://doi.org/10.1016/j.neuroimage.2010.07.073>
33. Di Liberto G.M., O’Sullivan J.A., Lalor E.C. 2015) **Low-Frequency Cortical Entrainment to Speech Reflects Phoneme-Level Processing** *Curr. Biol* **25**:2457–2465 <https://doi.org/10.1016/j.cub.2015.08.030>
34. Holdgraf C.R., Rieger J.W., Micheli C., Martin S., Knight R.T., Theunissen F.E. 2017) **Encoding and Decoding Models in Cognitive Electrophysiology** *Front. Syst. Neurosci* **11** <https://doi.org/10.3389/fnsys.2017.00061>
35. Li Y., Anumanchipalli G.K., Mohamed A., Chen P., Carney L.H., Lu J., Wu J., Chang E.F. 2023) **Dissecting neural computations in the human auditory pathway using deep neural networks for speech** *Nat. Neurosci.* :1–13 <https://doi.org/10.1038/s41593-023-01468-4>
36. Granger C.W.J. 1969) **Investigating Causal Relations by Econometric Models and Cross-spectral Methods** *Econometrica* **37**:424–438 <https://doi.org/10.2307/1912791>
37. Geweke J. 1982) **Measurement of Linear Dependence and Feedback between Multiple Time Series** *J. Am. Stat. Assoc* **77**:304–313 <https://doi.org/10.1080/01621459.1982.10477803>
38. Magee L. 1990) **R² Measures Based on Wald and Likelihood Ratio Joint Significance Tests** *Am. Stat* **44**:250–253 <https://doi.org/10.1080/00031305.1990.10475731>
39. Crosse M.J., Di Liberto G.M., Bednar A., Lalor E.C. 2016) **The Multivariate Temporal Response Function (mTRF) Toolbox: A MATLAB Toolbox for Relating Neural Signals to Continuous Stimuli** *Front. Hum. Neurosci* **10** <https://doi.org/10.3389/fnhum.2016.00604>
40. Friston K.J., Holmes A.P., Worsley K.J., Poline J. -P., Frith C.D., Frackowiak R.S.J. 1994) **Statistical parametric maps in functional imaging: A general linear approach** *Hum. Brain Mapp* **2**:189–210 <https://doi.org/10.1002/hbm.460020402>
41. Barnett L., Seth A.K. 2014) **The MVGC multivariate Granger causality toolbox: A new approach to Granger-causal inference** *J. Neurosci. Methods* **223**:50–68 <https://doi.org/10.1016/j.jneumeth.2013.10.018>
42. Penny W.D., Stephan K.E., Mechelli A., Friston K.J. 2004) **Comparing dynamic causal models** *NeuroImage* **22**:1157–1172 <https://doi.org/10.1016/j.neuroimage.2004.03.026>
43. Cakan C., Jajcay N., Obermayer K. 2023) **neurolib: A Simulation Framework for Whole-Brain Neural Mass Modeling** *Cogn. Comput* **15**:1132–1152 <https://doi.org/10.1007/s12559-021-09931-9>

44. Honey C.J., Sporns O., Cammoun L., Gigandet X., Thiran J.P., Meuli R., Hagmann P. 2009) **Predicting human resting-state functional connectivity from structural connectivity** *Proc. Natl. Acad. Sci* **106**:2035–2040 <https://doi.org/10.1073/pnas.0811168106>
45. Smith S.M., Miller K.L., Salimi-Khorshidi G., Webster M., Beckmann C.F., Nichols T.E., Ramsey J.D., Woolrich M.W. 2011) **Network modelling methods for FMRI** *NeuroImage* **54**:875–891 <https://doi.org/10.1016/j.neuroimage.2010.08.063>
46. Chen X. 2023) **xiaohuichen88/Graphical-Lasso** *GitHub*
47. Friedman J., Hastie T., Tibshirani R. 2008) **Sparse inverse covariance estimation with the graphical lasso** *Biostatistics* **9**:432–441 <https://doi.org/10.1093/biostatistics/kxm045>
48. Nentwich M., Leszczynski M., Russ B.E., Hirsch L., Markowitz N., Sapru K., Schroeder C.E., Mehta A.D., Bickel S., Parra L.C. 2023) **Semantic novelty modulates neural responses to visual change across the human brain** *Nat. Commun* **14**:2910 <https://doi.org/10.1038/s41467-023-38576-5>
49. Vanderwal T., Kelly C., Eilbott J., Mayes L.C., Castellanos F.X. 2015) **Inscapes : A movie paradigm to improve compliance in functional magnetic resonance imaging** *NeuroImage* **122**:222–232 <https://doi.org/10.1016/j.neuroimage.2015.07.069>
50. Chamma A., Frau-Pascual A., Rothberg A., Abadie A., Abraham A., Gramfort A., Savio A., Cionca A., Thual A., Kodibagkar A., et al. 2024) **nilearn** *Zenodo* <https://doi.org/10.5281/zenodo.10948303>
51. Gao R., van den Brink R.L., Pfeffer T., Voytek B. 2020) **Neuronal timescales are functionally dynamic and shaped by cortical microarchitecture** *eLife* **9**:e61277 <https://doi.org/10.7554/eLife.61277>
52. Gao R., Voytek B., Olayinka T. 2020) **rdgao/field-echos: post-publication** *Zenodo* <https://doi.org/10.5281/zenodo.4362645>
53. Glasser M.F., Coalson T.S., Robinson E.C., Hacker C.D., Harwell J., Yacoub E., Ugurbil K., Andersson J., Beckmann C.F., Jenkinson M., et al. 2016) **A multi-modal parcellation of human cerebral cortex** *Nature* **536**:171–178 <https://doi.org/10.1038/nature18933>
54. Markello R., Hansen J., Liu Z.-Q., Bazinet V., Shafiei G., Suarez L., Mišić B. 2024) **neuromaps: structural and functional interpretation of brain maps** *Zenodo* <https://doi.org/10.5281/zenodo.10607923>
55. Markello R.D., Hansen J.Y., Liu Z.-Q., Bazinet V., Shafiei G., Suárez L.E., Blostein N., Seidlitz J., Baillet S., Satterthwaite T.D., et al. 2022) **neuromaps: structural and functional interpretation of brain maps** *Nat. Methods* **19**:1472–1479 <https://doi.org/10.1038/s41592-022-01625-w>
56. Robinson E.C., Garcia K., Glasser M.F., Chen Z., Coalson T.S., Makropoulos A., Bozek J., Wright R., Schuh A., Webster M., et al. 2018) **Multimodal surface matching with higher-order smoothness constraints** *NeuroImage* **167**:453–465 <https://doi.org/10.1016/j.neuroimage.2017.10.037>
57. Robinson E.C., Jbabdi S., Glasser M.F., Andersson J., Burgess G.C., Harms M.P., Smith S.M., Van Essen D.C., Jenkinson M. 2014) **MSM: A new flexible framework for Multimodal Surface Matching** *NeuroImage* **100**:414–426 <https://doi.org/10.1016/j.neuroimage.2014.05.069>

58. Desikan R.S., Ségonne F., Fischl B., Quinn B.T., Dickerson B.C., Blacker D., Buckner R.L., Dale A.M., Maguire R.P., Hyman B.T., et al. 2006) **An automated labeling system for subdividing the human cerebral cortex on MRI scans into gyral based regions of interest** *NeuroImage* **31**:968–980 <https://doi.org/10.1016/j.neuroimage.2006.01.021>
59. Wang X.-J. 2020) **Macroscopic gradients of synaptic excitation and inhibition in the neocortex** *Nat. Rev. Neurosci* **21**:169–178 <https://doi.org/10.1038/s41583-020-0262-x>
60. Cole M.W., Bassett D.S., Power J.D., Braver T.S., Petersen S.E. 2014) **Intrinsic and Task-Evoked Network Architectures of the Human Brain** *Neuron* **83**:238–251 <https://doi.org/10.1016/j.neuron.2014.05.014>
61. Buzsáki G. 2019) **The Brain from Inside Out** Oxford University Press
62. Leszczyński M., Barczak A., Kajikawa Y., Ulbert I., Falchier A.Y., Tal I., Haegens S., Melloni L., Knight R.T., Schroeder C.E. 2020) **Dissociation of broadband high-frequency activity and neuronal firing in the neocortex** *Sci. Adv* **6**:eabb0977 <https://doi.org/10.1126/sciadv.abb0977>
63. Leszczynski M., Bickel S., Nentwich M., Russ B.E., Parra L., Lakatos P., Mehta A., Schroeder C.E. 2023) **Saccadic modulation of neural excitability in auditory areas of the neocortex** *Curr. Biol* <https://doi.org/10.1016/j.cub.2023.02.018>
64. Leszczynski M., Chaieb L., Staudigl T., Enkirch S.J., Fell J., Schroeder C.E. 2021) **Neural activity in the human anterior thalamus during natural vision** *Sci. Rep* **11**:17480 <https://doi.org/10.1038/s41598-021-96588-x>
65. Churchland M.M., Yu B.M., Cunningham J.P., Sugrue L.P., Cohen M.R., Corrado G.S., Newsome W.T., Clark A.M., Hosseini P., Scott B.B., et al. 2010) **Stimulus onset quenches neural variability: a widespread cortical phenomenon** *Nat. Neurosci* **13**:369–378 <https://doi.org/10.1038/nn.2501>
66. Arazi A., Yeshurun Y., Dinstein I. 2019) **Neural Variability Is Quenched by Attention** *J. Neurosci* **39**:5975–5985 <https://doi.org/10.1523/JNEUROSCI.0355-19.2019>
67. Arazi A., Censor N., Dinstein I. 2017) **Neural Variability Quenching Predicts Individual Perceptual Abilities** *J. Neurosci* **37**:97–109 <https://doi.org/10.1523/JNEUROSCI.1671-16.2016>
68. Mukamel R., Gelbard H., Arieli A., Hasson U., Fried I., Malach R. 2005) **Coupling Between Neuronal Firing, Field Potentials, and fMRI in Human Auditory Cortex** *Science* **309**:951–954 <https://doi.org/10.1126/science.1110913>
69. Huth A.G., de Heer W.A., Griffiths T.L., Theunissen F.E., Gallant J.L. 2016) **Natural speech reveals the semantic maps that tile human cerebral cortex** *Nature* **532**:453–458 <https://doi.org/10.1038/nature17637>
70. Nishimoto S., Vu A.T., Naselaris T., Benjamini Y., Yu B., Gallant J.L. 2011) **Reconstructing Visual Experiences from Brain Activity Evoked by Natural Movies** *Curr. Biol* **21**:1641–1646 <https://doi.org/10.1016/j.cub.2011.08.031>
71. Broderick M.P., Anderson A.J., Di Liberto G.M., Crosse M.J., Lalor E.C. 2018) **Electrophysiological Correlates of Semantic Dissimilarity Reflect the Comprehension of Natural, Narrative Speech** *Curr. Biol* **28**:803–809 <https://doi.org/10.1016/j.cub.2018.01.080>

72. Fair D.A., Schlaggar B.L., Cohen A.L., Miezin F.M., Dosenbach N.U.F., Wenger K.K., Fox M.D., Snyder A.Z., Raichle M.E., Petersen S.E. 2007) **A method for using blocked and event-related fMRI data to study “resting state” functional connectivity** *NeuroImage* **35**:396–405 <https://doi.org/10.1016/j.neuroimage.2006.11.051>
73. Rissman J., Gazzaley A., D’Esposito M. 2004) **Measuring functional connectivity during distinct stages of a cognitive task** *NeuroImage* **23**:752–763 <https://doi.org/10.1016/j.neuroimage.2004.06.035>
74. Ryali S., Supekar K., Chen T., Menon V. 2011) **Multivariate dynamical systems models for estimating causal interactions in fMRI** *NeuroImage* **54**:807–823 <https://doi.org/10.1016/j.neuroimage.2010.09.052>

Author information

Maximilian Nentwich

The Feinstein Institutes for Medical Research, Northwell Health, Manhasset, United States
ORCID iD: [0000-0002-9306-7591](https://orcid.org/0000-0002-9306-7591)

For correspondence: max.nentwich@gmail.com

Marcin Leszczynski

Departments of Psychiatry and Neurology, Columbia University College of Physicians and Surgeons, New York, United States, Translational Neuroscience Lab Division, Center for Biomedical Imaging and Neuromodulation, Nathan Kline Institute, Orangeburg, United States, Cognitive Science Department, Institute of Philosophy, Jagiellonian University, Kraków, Poland

Charles E Schroeder

Departments of Psychiatry and Neurology, Columbia University College of Physicians and Surgeons, New York, United States, Translational Neuroscience Lab Division, Center for Biomedical Imaging and Neuromodulation, Nathan Kline Institute, Orangeburg, United States

Stephan Bickel

The Feinstein Institutes for Medical Research, Northwell Health, Manhasset, United States, Departments of Neurology and Neurosurgery, Zucker School of Medicine at Hofstra/Northwell, Hempstead, United States, Center for Biomedical Imaging and Neuromodulation, Nathan Kline Institute, Orangeburg, United States
ORCID iD: [0000-0001-5265-2447](https://orcid.org/0000-0001-5265-2447)

Lucas C Parra

Department of Biomedical Engineering, The City College of New York, New York, United States
ORCID iD: [0000-0003-4667-816X](https://orcid.org/0000-0003-4667-816X)

Editors

Reviewing Editor

Rick Adams

University College London, London, United Kingdom

Senior Editor

Andre Marquand

Radboud University Nijmegen, Nijmegen, Netherlands

Reviewer #1 (Public review):

This manuscript presents an interesting new framework (VARX) for simultaneously quantifying effective connectivity in brain activity during sensory stimulation and how that brain activity is being driven by that sensory stimulation. The core idea is to combine the Vector Autoregressive model that is often used to infer Granger-causal connectivity in brain data with an encoding model that maps the features of a sensory stimulus to that brain data. The authors do a nice job of explaining the framework. And then they demonstrate its utility through some simulations and some analysis of real intracranial EEG data recorded from subjects as they watched movies. They infer from their analyses that the functional connectivity in these brain recordings is essentially unaltered during movie watching, that accounting for the driving movie stimulus can protect one against misidentifying brain responses to the stimulus as functional connectivity, and that recurrent brain activity enhances and prolongs the putative neural responses to a stimulus.

This manuscript presents an interesting new framework (VARX) for simultaneously quantifying effective connectivity in brain activity during sensory stimulation and how that brain activity is being driven by that sensory stimulation. Overall, I thought this was an interesting manuscript with some rich and intriguing ideas. That said, I had some concerns also - one potentially major - with the inferences drawn by the authors on the analyses that they carried out.

Main comments:

(1) My primary concern with the way the manuscript is written right now relates to the inferences that can be drawn from the framework. In particular, the authors want to assert that, by incorporating an encoding model into their framework, they can do a better job of accounting for correlated stimulus-driven activity in different brain regions, allowing them to get a clearer view of the underlying innate functional connectivity of the brain. Indeed, the authors say that they want to ask "whether, after removing stimulus-induced correlations, the intrinsic dynamic itself is preserved". This seems a very attractive idea indeed. However, it seems to hinge critically on the idea of fitting an encoding model that fully explains all of the stimulus-driven activity. In other words, if one fits an encoding model that only explains some of the stimulus-driven response, then the rest of the stimulus-driven response still remains in the data and will be correlated across brain regions and will appear as functional connectivity in the ongoing brain dynamics - according to this framework. This residual activity would thus be misinterpreted. In the present work, the authors parameterize their stimulus using fixation onsets, film cuts, and the audio envelope. All of these features seem reasonable and valid. However, they surely do not come close to capturing the full richness of the stimuli, and, as such, there is surely a substantial amount of stimulus-driven brain activity that is not being accounted for by their "B" model and that is being absorbed into their "A" model and misinterpreted as intrinsic connectivity. This seems to me to be a major limitation of the framework. Indeed, the authors flag this concern themselves by (briefly) raising the issue in the first paragraph of their caveats section. But I think it warrants much more attention and discussion.

(2) Related to the previous comment, the authors make what seems to me to be a complex and important point on page 6 (of the pdf). Specifically, they say "Note that the extrinsic effects captured with filters B are specific (every stimulus dimension has a specific effect on each brain area), whereas the endogenous dynamic propagates this initial effect to all connected brain areas via matrix A, effectively mixing and adding the responses of all stimulus dimensions. Therefore, this factorization separates stimulus-specific effects from the

shared endogenous dynamic." It seems to me that the interpretation of the filter B (which is analogous to the "TRF") for the envelope, say, will be affected by the fact that the matrix A is likely going to be influenced by all sorts of other stimulus features that are not included in the model. In other words, residual stimulus-driven correlations that are captured in A might also distort what is going on in B, perhaps. So, again, I worry about interpreting the framework unless one can guarantee a near-perfect encoding model that can fully account for the stimulus-driven activity. I'd love to hear the authors' thoughts on this. (On this issue - the word "dominates" on page 12 seems very strong.)

(3) Regarding the interpretation of the analysis of connectivity between movies and rest... that concludes that the intrinsic connectivity pattern doesn't really differ. This is interesting. But it seems worth flagging that this analysis doesn't really account for the specific dynamics in the network that could differ quite substantially between movie watching and rest, right? At the moment, it is all correlational. But the dynamics within the network could be very different between stimulation and rest I would have thought.

(4) I didn't really understand the point of comparing the VARX connectivity estimate with the sparse-inverse covariance method (Figure 2D). What was the point of this? What is a reader supposed to appreciate from it about the validity or otherwise of the VARX approach?

(5) I think the VARX model section could have benefitted a bit from putting some dimensions on some of the variables. In particular, I struggled a little to appreciate the dimensionality of A. I am assuming it has to involve both time lags AND electrode channels so that you can infer Granger causality (by including time) between channels. Including a bit more detail on the dimensionality and shape of A might be helpful for others who want to implement the VARX model.

(6) A second issue I had with the inferences drawn by the authors was a difficulty in reconciling certain statements in the manuscript. For example, in the abstract, the authors write "We find that the recurrent connectivity during rest is largely unaltered during movie watching." And they also write that "Failing to account for ... exogenous inputs, leads to spurious connections in the intrinsic "connectivity".

<https://doi.org/10.7554/eLife.104996.1.sa1>

Reviewer #2 (Public review):

Summary:

The authors apply the recently developed VARX model, which explicitly models intrinsic dynamics and the effect of extrinsic inputs, to simulated data and intracranial EEG recordings. This method provides a directed method of 'intrinsic connectivity'. They argue this model is better suited to the analysis of task neuroimaging data because it separates the intrinsic and extrinsic activity. They show: that intrinsic connectivity is largely unaltered during a movie-watching task compared to eyes open rest; intrinsic noise is reduced in the task; and there is intrinsic directed connectivity from sensory to higher-order brain areas.

Strengths:

- (1) The paper tackles an important issue with an appropriate method.
- (2) The authors validated their method on data simulated with a neural mass model.
- (3) They use intracranial EEG, which provides a direct measure of neuronal activity.
- (4) Code is made publicly available and the paper is written well.

Weaknesses:

It is unclear whether a linear model is adequate to describe brain data. To the author's credit, they discuss this in the manuscript. Also, the model presented still provides a useful and computationally efficient method for studying brain data - no model is 'the truth'.

Appraisal of whether the authors achieve their aims:

As a methodological advancement highlighting a limitation of existing approaches and presenting a new model to overcome it, the authors achieve their aim. Generally, the claims/conclusions are supported by the results.

The wider neuroscience claims regarding the role of intrinsic dynamics and external inputs in affecting brain data could benefit from further replication with another independent dataset and in a variety of tasks - but I understand if the authors wanted to focus on the method rather than the neuroscientific claims in this manuscript.

Impact:

The authors propose a useful new approach that solves an important problem in the analysis of task neuroimaging data. I believe the work can have a significant impact on the field.

<https://doi.org/10.7554/eLife.104996.1.sa0>